American Mineralogist, Volume 77, pages 76–84, 1992

Tetrahedral-site occupancies in reedmergnerite and synthetic boron albite ($NaBSi_3O_8$)

MICHAEL E. FLEET
Department of Geology, University of Western Ontario, London, Ontario N6A 5B7, Canada

ABSTRACT

The structures of three B-substituted albite samples ($NaBSi_3O_8$), including reedmergnerite from Utah and low and high synthetic boron albite, have been refined at room temperature with single-crystal X-ray intensities. For reedmergnerite, $R = 0.019$, the structure is ideally ordered with B in the T_10 site, and the electron density distribution at the Na position is anisotropic as in low albite and low gallium albite. Average T-O distances are T_10 [1.472(1)], T_1m [1.611(1)], T_20 [1.615(1)], T_2m [1.619(1) Å]. The structure of low boron albite refined to $R = 0.027$. Average T-O distances and B site occupancies are T_10 [1.497(2), 0.805(1)], T_1m [1.606(1), 0.014(1)], T_20 [1.593(1), 0.135(1)], T_2m [1.610(1) Å, 0.046(1)]. The structure of high boron albite refined similarly to $R = 0.037$, T_10 [1.571(2), 0.289(3)], T_1m [1.598(2), 0.058(3)], T_20 [1.553(2), 0.384(3)], T_2m [1.574(2) Å, 0.269(3)].

Average T-O distances for reedmergnerite and boron albite exhibit an almost linear correlation with site occupancies of B (t_iB). The tetrahedral-site ordering sequences of $t_10 \gg t_20 \gg t_2m > t_1m$ in low boron albite and $t_20 > t_10 \approx t_2m > t_1m$ in high boron albite are very unusual compared with albite but do correlate with stereochemical features. High boron albite is antiordered with $(t_10 + t_1m) < (t_20 + t_2m)$. The order-disorder transformation in boron albite appears to occur within the temperature range 500–550 °C at $P_{H_2O} \approx 1$ kbar.

INTRODUCTION

The triclinic alkali feldspars (space group $C\bar{1}$) have four nonequivalent tetrahedral sites for Si and Al, designated T_10, T_1m, T_20, and T_2m, with occupancies of Al (or trivalent atoms) designated t_10, t_1m, t_20, and t_2m, respectively. As reviewed by Fleet (1991a), tetrahedral-site ordering closely approximates to $t_10 > t_1m \approx t_20 \approx t_2m < 0.25$ in high albite, $t_10 \rightarrow 1$, $t_1m \approx t_20 \approx t_2m \rightarrow 0$ in low albite, and $t_10 \rightarrow 1$, $t_1m \geq t_20 \approx t_2m \rightarrow 0$ in triclinic K-rich feldspars.

Recent studies (Burns and Fleet, 1990; Fleet, 1990, 1991a, 1991b; Kroll et al., 1991) have used isostructural analogues of albite with Ga substitution for Al or Ge substitution for Si as an additional (chemical) dimension in the study of order-disorder in alkali feldspar. The Rietveld study of Burns and Fleet (1990) determined the order-disorder transformation in Ga-substituted albite ($NaGaSi_3O_8$, hereafter referred to as gallium albite) to be continuous with a well-defined region of intermediate structure and an ordering path of $t_10 \rightarrow 1$, $t_1m \approx t_20 \approx t_2m \rightarrow 0$. Single-crystal X-ray studies revealed a largely ordered structure for low gallium albite (Swanson, 1986; Fleet, 1991a). Also, within the stability field for low gallium albite, Ga remains largely ordered in a matrix of disordered aluminum-silicon feldspar (Fleet, 1991b). Curiously, the preferred sequence of tetrahedral sites in gallium albite and aluminum-gallium albite is $t_10 \gg t_20 \approx t_2m > t_1m \rightarrow 0.0$ (Fleet, 1991a, 1991b). The Ge-substituted albite ($NaAlGe_3O_8$, hereafter referred to as germanium albite) presently synthesized has disordered (intermediate and high) structures with the unusual site preference to $t_1m > t_10$ (Fleet, 1991a; Kroll et al., 1991). Both Ga- and Ge-substituted albites provide examples of antiordered feldspars (cf. Thompson et al., 1974). Fleet (1990, 1991a) suggested that the tetrahedral-site ordering in alkali feldspar is promoted by the distinctive stereochemistries of the T_10 and T_1m sites, which are imposed by spatial accommodation of the Na cation within the feldspar framework. Site preference is determined by favorable charge or valence electron distribution, minimization of T-Na repulsion, and spatial accommodation. It was noted that the preference for the T_10 site increases in the sequence $Fe^{3+} > Ga > B > Al$, which correlates with the absolute difference in size with Si.

Reedmergnerite ($NaBSi_3O_8$) occurs as an authigenic mineral in black oil shale and brown dolomitic rock of the Green River Formation (Milton et al., 1954, 1960) and also in peralkaline pegmatites from Tadzhikistan (Dusmatov et al., 1967). The crystal structure, isostructural with low albite, was confirmed and refined using film intensities by Appleman and Clark (1965), who reported an ordered structure with no apparent anisotropy of the electron density distribution at the Na atom position (cf. Fleet, 1991a). Synthetic reedmergnerite (hereafter referred to as boron albite) has been studied by Eugster and McIver (1959), Bruno and Pentinghaus (1974), Kimata (1977), Ostertag (1980), and Mason (1980a,

0003–004X/92/0102–0076$02.00

TABLE 1. Experimental details

	Reedmergnerite Utah	Low boron albite Gb100	High boron albite Gb87
Crystal size (mm)	0.29 × 0.20 × 0.15	0.12 × 0.19 × 0.07	0.16 × 0.07 × 0.19
Unit-cell parameters			
a (Å)	7.8388(9)	7.852(3)	7.910(2)
b	12.3730(10)	12.350(4)	12.336(2)
c	6.8082(7)	6.806(1)	6.820(1)
α (°)	93.324(8)	93.37(2)	93.54(2)
β	116.381(9)	116.30(3)	116.13(2)
γ	92.014(8)	91.58(3)	90.60(2)
θ range (°) of reflections	17.7–31.6	17.6–21.8	17.5–31.4
Intensity data collection			
Method	θ-2θ	ω	ω
Reflections, type	$\pm h \pm k \pm l$	$\pm h \pm k \pm l$	$\pm h \pm k \pm l$
Number	5180	3414	3458
2θ limit (°)	70	60	60
Transmission factors	0.87–0.90	0.86–0.94	0.87–0.94
Final data list			
Total reflections	2590	1707	1729
Number unobserved	219	416	277
Final refinement			
R (unweighted, %)	1.9	2.7	3.7
R_w (weighted, %)	2.5	2.0	3.0
Extinction (g, $\times 10^4$)	0.91(5)	—	0.28(6)

1980b). Eugster and McIver (1959) synthesized low boron albite at 300–500 °C, 2.0 kbar, and Bruno and Pentinghaus (1974) reported unit-cell parameters for high boron albite synthesized at 700 °C, 4 bars. Kimata (1977) suggested that the order-disorder transformation occurred in the range 500–700 °C, but this was not well constrained. Mason (1980a, 1980b) reported that the morphology of boron albite grown by hydrothermal synthesis changes systematically with time and rate of change of B-Si order. Also, in contrast to the behavior of albite, ordering in boron albite is insensitive to composition of the coexisting fluid and may occur through recrystallization rather than by solid state diffusion.

This paper describes the tetrahedral-site ordering and electron density distribution at the Na atom position in reedmergnerite from the Green River Formation and low and high structure boron albite, based on structures refined using single-crystal X-ray diffraction data.

EXPERIMENTAL PROCEDURES

Materials

Reedmergnerite from the type locality (Duchesne County, Utah, Milton et al., 1960) was obtained from the National Museum of Natural History, Smithsonian Institution (catalogue number NMNH 140710). Crystals of low and high boron albite ($NaBSi_3O_8$) were grown hydrothermally, using a standard cold-seal reaction vessel, and quenched in air and H_2O. Starting material was a mechanical mixture of purified SiO_2 and analytical grade Na_2CO_3 and H_3BO_3 in the stoichiometric proportion for $NaBSi_3O_8$. Charges consisted of 0.05 g boron albite mixture and 0.02 cm^3 of deionized H_2O in a sealed Au capsule about 4 cm in length. For low boron albite, the capsule was heated at 462 °C and 1.8 kbar for 6 d. The products consisted of low boron albite and minor quartz. For high boron albite, the capsule was heated at 850 °C and 1.6 kbar for 1 h (to achieve complete melting), cooled and maintained overnight at 580 °C and 0.8 kbar, and then cooled stepwise and maintained at 478 °C and 0.5 kbar for 3 d. The products consisted of high boron albite and minor quartz.

Structure refinements

Single-crystal measurements were made with an Enraf-Nonius CAD-4F diffractometer, using graphite-monochromatized Mo*Kα* X-radiation. Structure refinements followed Fleet (1991a), and experimental details are given in Table 1. The ideal formula ($NaBSi_3O_8$) was assumed for all three crystals, and scattering factors for neutral atomic species and values of f' and f'' were taken, respectively, from Tables 2.2B and 2.3.1 of the *International Tables for X-ray Crystallography* (1974). Final parameters are given in Tables 2 and 3, and observed and calculated structure factors are given in Table 4.[1]

DISCUSSION

Selected bond distances and bond angles for reedmergnerite and low and high boron albite (synthetic reedmergnerite) are given in Tables 5 and 6, tetrahedral-site occupancies are given in Table 7, and the stereochemical environments of Na are represented in Figures 1 and 2. The low and high boron albite were not chemically analyzed to confirm stoichiometric proportions. However, with allowance for the effects of order-disorder, their unit-cell parameters are closely comparable to the parameters for synthetic reedmergnerite from other studies employing different methods of sample preparation (cf. Kimata,

---

[1] A copy of Table 4 may be ordered as Document AM-92-486 from the Business Office, Mineralogical Society of America, 1130 Seventeenth Street NW, Suite 330, Washington, DC 20036, U.S.A. Please remit $5.00 in advance for the microfiche.

TABLE 2. Positional and isotropic thermal parameters (Å^2)

	x	y	z	B_{eq}
Reedmergnerite, Utah				
Na	0.2582(1)	0.0075(1)	0.1330(1)	1.54(1)
$T_{1}0$	0.0121(2)	0.1616(1)	0.2215(2)	0.51(2)
$T_{1}m$	0.00585(4)	0.80969(3)	0.20966(5)	0.39(1)
$T_{2}0$	0.70278(4)	0.10177(2)	0.32033(5)	0.40(1)
$T_{2}m$	0.68471(4)	0.86450(2)	0.35438(5)	0.38(1)
$O_{A}1$	0.0077(1)	0.1363(1)	0.0037(1)	0.65(2)
$O_{A}2$	0.5931(1)	0.9813(1)	0.2757(1)	0.54(2)
$O_{B}0$	0.8449(1)	0.0989(1)	0.2116(1)	0.78(2)
$O_{B}m$	0.8161(1)	0.8349(1)	0.2336(1)	0.82(2)
$O_{C}0$	0.0068(1)	0.2765(1)	0.2733(1)	0.66(2)
$O_{C}m$	0.0290(1)	0.6798(1)	0.2060(1)	0.68(2)
$O_{D}0$	0.1904(1)	0.1186(1)	0.3829(1)	0.77(2)
$O_{D}m$	0.1921(1)	0.8680(1)	0.4171(1)	0.78(2)
Low boron albite, Gb100 ($NaBSi_3O_8$)				
Na	0.2640(1)	0.0079(1)	0.1335(2)	2.89(2)
$T_{1}0$	0.0083(2)	0.1640(1)	0.2213(2)	0.68(2)
$T_{1}m$	0.0075(1)	0.8097(1)	0.2158(1)	0.55(1)
$T_{2}0$	0.7021(1)	0.1030(1)	0.3199(1)	0.50(1)
$T_{2}m$	0.6862(1)	0.8674(1)	0.3546(1)	0.56(1)
$O_{A}1$	0.0061(2)	0.1370(1)	0.9990(2)	1.12(4)
$O_{A}2$	0.5961(2)	0.9839(1)	0.2765(2)	0.90(3)
$O_{B}0$	0.8392(2)	0.1022(1)	0.2092(2)	1.36(4)
$O_{B}m$	0.8177(2)	0.8363(1)	0.2365(2)	1.21(4)
$O_{C}0$	0.0098(2)	0.2807(1)	0.2749(2)	1.13(4)
$O_{C}m$	0.0298(2)	0.6801(1)	0.2110(2)	1.09(4)
$O_{D}0$	0.1901(2)	0.1174(1)	0.3834(2)	1.12(4)
$O_{D}m$	0.1917(2)	0.8680(1)	0.4209(2)	1.18(4)
High boron albite, Gb87 ($NaBSi_3O_8$)				
Na	0.2823(2)	0.0075(2)	0.1356(3)	7.08(6)
$T_{1}0$	0.0093(1)	0.1681(1)	0.2203(2)	0.78(2)
$T_{1}m$	0.0093(1)	0.8100(1)	0.2305(1)	0.82(2)
$T_{2}0$	0.6995(2)	0.1056(1)	0.3219(2)	0.80(3)
$T_{2}m$	0.6910(1)	0.8758(1)	0.3556(2)	0.75(2)
$O_{A}1$	0.0048(2)	0.1390(1)	0.9876(3)	1.49(5)
$O_{A}2$	0.6050(2)	0.9890(1)	0.2783(3)	1.21(4)
$O_{B}0$	0.8264(2)	0.1108(1)	0.2042(3)	1.78(5)
$O_{B}m$	0.8197(2)	0.8392(1)	0.2452(3)	1.72(5)
$O_{C}0$	0.0189(2)	0.2922(1)	0.2810(3)	1.43(4)
$O_{C}m$	0.0294(2)	0.6810(1)	0.2215(3)	1.39(4)
$O_{D}0$	0.1921(2)	0.1134(1)	0.3866(3)	1.42(4)
$O_{D}m$	0.1895(2)	0.8681(1)	0.4281(3)	1.54(4)

Note: $B_{eq} = \frac{4}{3} \Sigma_i \Sigma_j \beta_{ij} \mathbf{a}_i \cdot \mathbf{a}_j$.

TABLE 3. Anisotropic thermal parameters ($\times 10^2$ Å^2)

	B_{11}	B_{22}	B_{33}	B_{12}	B_{13}	B_{23}
Reedmergnerite, Utah						
Na	93(2)	190(2)	154(2)	21(2)	41(2)	−61(2)
$T_{1}0$	59(4)	51(4)	48(4)	1(3)	27(3)	5(3)
$T_{1}m$	47(1)	39(1)	34(1)	14(1)	20(1)	8(1)
$T_{2}0$	43(1)	33(1)	43(1)	7(1)	18(1)	5(1)
$T_{2}m$	42(1)	34(1)	42(1)	11(1)	21(1)	8(1)
$O_{A}1$	98(3)	67(3)	40(3)	15(2)	40(2)	12(2)
$O_{A}2$	51(3)	35(3)	72(3)	9(2)	23(2)	14(2)
$O_{B}0$	83(3)	71(3)	104(3)	−19(2)	68(3)	−12(2)
$O_{B}m$	76(3)	99(3)	96(3)	25(2)	61(3)	10(3)
$O_{C}0$	68(3)	41(3)	96(3)	1(2)	46(3)	−4(2)
$O_{C}m$	71(3)	45(3)	73(3)	24(2)	16(2)	9(2)
$O_{D}0$	81(3)	93(3)	43(3)	39(2)	12(2)	10(2)
$O_{D}m$	80(3)	85(3)	49(3)	−1(2)	10(2)	−5(2)
Low boron albite, Gb100 ($NaBSi_3O_8$)						
Na	180(4)	364(5)	262(5)	37(4)	62(4)	−141(4)
$T_{1}0$	84(5)	73(5)	49(5)	13(4)	31(4)	7(4)
$T_{1}m$	62(2)	54(2)	61(2)	12(2)	36(2)	11(2)
$T_{2}0$	59(2)	40(2)	50(2)	2(2)	23(2)	3(2)
$T_{2}m$	58(2)	72(2)	49(2)	21(2)	32(2)	17(2)
$O_{A}1$	162(6)	109(6)	89(5)	22(5)	76(5)	17(4)
$O_{A}2$	89(5)	79(5)	101(5)	11(4)	39(4)	21(4)
$O_{B}0$	162(6)	116(6)	144(6)	−34(5)	89(5)	−20(5)
$O_{B}m$	114(6)	138(6)	136(6)	34(5)	76(5)	18(5)
$O_{C}0$	115(6)	119(6)	123(6)	18(5)	68(5)	19(5)
$O_{C}m$	122(6)	82(5)	107(6)	20(4)	36(5)	9(4)
$O_{D}0$	123(6)	121(6)	84(6)	34(5)	37(5)	7(4)
$O_{D}m$	122(6)	113(6)	97(6)	−4(5)	31(5)	0(5)
High boron albite, Gb87 ($NaBSi_3O_8$)						
Na	218(6)	1072(13)	613(10)	35(7)	62(6)	−568(9)
$T_{1}0$	96(4)	75(4)	59(4)	3(3)	32(3)	5(3)
$T_{1}m$	88(3)	75(3)	84(3)	14(2)	36(2)	19(2)
$T_{2}0$	77(5)	74(4)	71(4)	−1(3)	18(3)	−2(3)
$T_{2}m$	63(4)	95(4)	70(4)	23(3)	31(3)	19(3)
$O_{A}1$	217(8)	127(7)	116(7)	10(6)	85(6)	11(5)
$O_{A}2$	101(7)	121(7)	125(7)	11(5)	34(5)	21(5)
$O_{B}0$	189(8)	164(8)	182(8)	−51(6)	90(6)	−21(6)
$O_{B}m$	138(7)	181(8)	209(8)	33(6)	88(6)	8(6)
$O_{C}0$	127(7)	155(7)	159(7)	25(6)	73(6)	26(6)
$O_{C}m$	132(7)	105(7)	144(7)	16(5)	30(6)	1(5)
$O_{D}0$	152(7)	140(7)	117(7)	25(6)	42(6)	15(5)
$O_{D}m$	151(7)	132(7)	145(7)	−7(6)	37(6)	−1(6)

Note: Anisotropic temperature factors have the form $\exp[-\frac{1}{4}(B_{11}h^2a^{*2} + \ldots + 2B_{23}klb^*c^*\cos\alpha^*)]$.

1977; Bruno and Pentinghaus, 1974). The parameters quoted by Mason (1980b) are all for samples more ordered than the present low boron albite.

Refined structures

Refinement of the structures of reedmergnerite and boron albite was unexpectedly complicated. Following the procedure of Fleet (1991a), with the occupancies constrained by $\Sigma t_iB = 1.0$, all three refinements appeared to converge normally (albeit slowly). However, some disorder was computed for reedmergnerite [$t_10 = 0.896$, $t_1m = 0.039(3)$, $t_20 = 0.028(3)$, $t_2m = 0.037(3)$], and the thermal ellipsoids for the T_10 site were anomalously large (B_{eq} = 1.47, 1.54, 1.19 e·Å^3 for reedmergnerite, low boron albite, and high boron albite, respectively) compared with values for B in tetrahedral coordination in borates (e.g., Ghose and Wan, 1979). The thermal parameters for T_10 were not strongly correlated with the occupancies, but the least-squares procedure clearly was placing too much electron density (in the form of Si atoms) at the T_10 site. This aberration was attributed to the contribution of valence electrons to the electron density distribution. For the ideally ordered structure, the electron density at the positions whose occupancies are being refined (T_1m, T_20, T_2m) is too high relative to the density at the O atom positions, and the least-squares procedure attempts to reduce it by replacing Si atoms by B. Although there is good X-ray scattering contrast between Si and B, the X-ray site-occupancy refinements of the present structures are limited by the lack of X-ray scattering factors for the partially charged atoms. Unfortunately, the quantitative estimation of atomic charge and deformation electron density remain controversial (e.g., Sasaki et al., 1980), and their contributions to the reedmergnerite structure would be appropriately considered in a future study.

Reedmergnerite, in fact, has an ordered structure to within resolution of the present methods, and this conclusion is demonstrated quite readily. The residual index (R) is minimized for the ordered structure; R decreases from 0.030 for the above refinement with occupancies to 0.019 for the ordered structure ($t_10B = 1.0$) and increases

TABLE 5. Selected interatomic distances (Å) and bond angles (°)

	Reedmergnerite	Low boron albite Gb100	High boron albite Gb87		Reedmergnerite	Low boron albite Gb100	High boron albite Gb87
Na-O_A1	2.454(1)	2.487(2)	2.607(2)	Na-O_Bm	3.118(1)	3.108(2)	3.124(3)
Na-O_A1	2.490(1)	2.533(2)	2.679(2)	Na-O_C0	—	—	3.215(2)
Na-O_A2	2.402(1)	2.379(1)	2.316(2)	Na-O_Cm	2.814(1)	2.794(2)	2.737(2)
Na-O_B0	2.403(1)	2.416(2)	2.457(2)	Na-O_Dm	2.864(1)	2.909(2)	3.028(2)
Na-O_D0	2.377(1)	2.389(2)	2.443(2)				
$T_1$0-O_A1	1.483(1)	1.522(1)	1.591(2)	$T_2$0-O_A2	1.636(1)	1.615(1)	1.563(2)
$T_1$0-O_B0	1.472(1)	1.481(2)	1.560(1)	$T_2$0-O_B0	1.588(1)	1.563(1)	1.540(2)
$T_1$0-O_C0	1.452(1)	1.464(2)	1.552(2)	$T_2$0-O_Cm	1.622(1)	1.598(1)	1.562(2)
$T_1$0-O_D0	1.482(1)	1.520(2)	1.582(1)	$T_2$0-O_Dm	1.614(1)	1.594(1)	1.546(2)
Average	1.472	1.497	1.571	Average	1.615	1.593	1.553
T_1m-O_A1	1.596(1)	1.600(1)	1.610(2)	T_2m-O_A2	1.647(1)	1.633(1)	1.577(2)
T_1m-O_Bm	1.606(1)	1.599(1)	1.590(1)	T_2m-O_Bm	1.617(1)	1.606(1)	1.565(2)
T_1m-O_Cm	1.624(1)	1.615(2)	1.601(2)	T_2m-O_C0	1.605(1)	1.595(1)	1.572(1)
T_1m-O_Dm	1.619(1)	1.610(1)	1.590(1)	T_2m-O_D0	1.608(1)	1.605(1)	1.582(2)
Average	1.611	1.606	1.598	Average	1.619	1.610	1.574

if as little as 0.1% disorder is introduced. Therefore, an ordered structure was assumed for reedmergnerite, and site occupancies were not included in the present refinement.

For low and high boron albite, atomic charge effects were compensated during refinement by lifting the constraint of $\Sigma t_i B = 1.0$ but retaining the total occupancy (Si + B) of each site at 1.0. For low and high boron albite, total Si cations pfu [Σ(Si)] refined to 2.79 and 2.75, respectively; they were less than 3.00 because the total reduction in electron density due to atomic charge is greater for Si than B. Compared with the aberrant refinements for low and high boron albite, *R* was reduced from 0.032 to 0.027 and from 0.042 to 0.037, respectively. The resulting tetrahedral-site preferences for boron albite, normalized to $\Sigma t_i Si = 3.0$ (Table 7), are qualitatively similar to those derived from the aberrant refinements [which were $t_1$0 = 0.705, t_1m = 0.053(3), $t_2$0 = 0.158(3), t_2m = 0.084(3), for low boron albite and $t_1$0 = 0.219, t_1m = 0.091(4), $t_2$0 = 0.397(4), t_2m = 0.294(4) for high boron albite].

It is emphasized that all of the presently discussed refinements for reedmergnerite and boron albite converged. The aberrant and accepted refinements differ in the method for estimating site occupancies. Site occupancies refined with the constraint $\Sigma t_i B = 1.0$ are reported in the text but are limited by lack of appropriate X-ray scattering factors. The presently accepted site occupancies result in significant reduction in *R* (cf. Hamilton, 1965), the commonly recognized criterion for acceptability of refinement.

The present refinement of the structure of reedmergnerite is very similar to that of Appleman and Clark (1965). Both studies show a fully ordered structure. The positional parameters agree to within 1 or 2 sd, and the isotropic thermal parameters are similar. The only significant difference is in the electron density distribution at the Na atom position, which the present study shows to be anisotropic (Figs. 1 and 2) as in low albite (e.g., Harlow and Brown, 1980) and low gallium albite (Fleet, 1991a).

Fleet (1991a) noted that, as a result of its accommodation within the feldspar framework, the Na atom in albite structures is relatively unconstrained transverse to the plane of the strongest Na-O bonds (Na-O_A2, Na-O_B0, and Na-O_D0; cf. Table 5, Figs. 1 and 2). Therefore, even in an ideally ordered albite structure, the thermal vibration is exaggerated in this transverse direction. Addition-

TABLE 6. O (T-O-T) bond angles in reedmergnerite, boron albite, and other alkali feldspars

	Reedmergnerite	Low boron albite Gb100	High boron albite Gb87	Reed-mergnerite 1	Low albite 2	Gallium albite 3	Germanium albite 3	Inter-mediate albite 4
$T_1$0-O_A1-T_1m	142.9(1)	142.8(1)	143.8(1)	143.1	141.5	137.9	139.5	142.7
$T_2$0-O_A2-T_2m	128.9(1)	129.5(1)	131.3(1)	128.7	129.7	130.7	125.2	129.8
$T_1$0-O_B0-$T_2$0	139.8(1)	140.1(1)	142.2(1)	140.5	139.8	134.9	132.8	140.4
T_1m-O_Bm-T_2m	158.2(1)	157.9(1)	157.4(1)	158.1	161.5	161.9	157.0	159.4
$T_1$0-O_C0-T_2m	125.1(1)	127.0(1)	128.8(1)	124.9	129.8	125.2	124.4	130.3
T_1m-O_Cm-$T_2$0	135.7(1)	135.2(1)	133.8(1)	135.9	135.8	138.1	131.3	134.7
$T_1$0-O_D0-T_2m	134.9(1)	134.2(1)	133.7(1)	135.4	133.9	131.8	130.8	134.9
T_1m-O_Dm-$T_2$0	146.4(1)	146.7(1)	147.6(1)	146.3	151.8	154.7	150.0	150.5
⟨$T_1$0-O-T⟩	135.7	136.0	137.1	136.0	136.3	132.5	131.9	137.1
⟨T_1m-O-T⟩	145.8	145.7	145.7	145.9	147.7	148.2	144.6	146.8
⟨$T_2$0-O-T⟩	137.7	137.9	138.7	137.9	139.3	139.6	134.8	138.9
⟨T_2m-O-T⟩	136.8	137.2	137.8	136.8	138.7	137.4	134.4	138.6

Note: 1 = Appleman and Clark (1965); 2 = Harlow and Brown (1980); 3 = Fleet (1991a); 4 = Phillips et al. (1989).

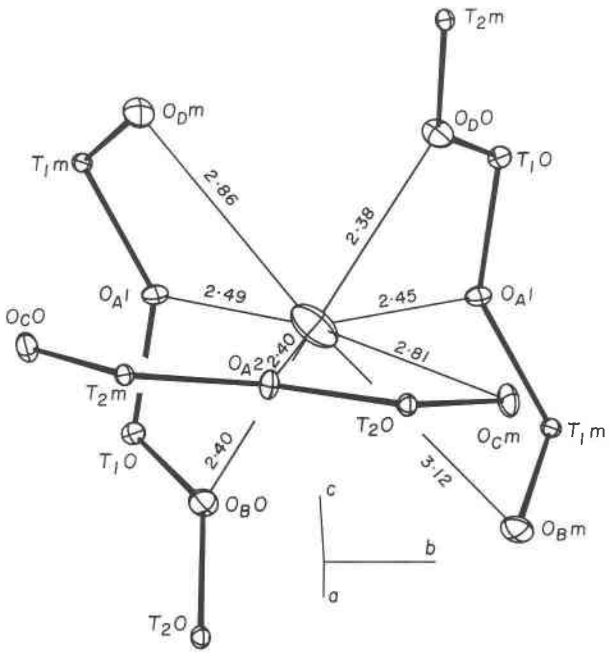

Fig. 1. Stereochemical environment of Na to 3.6 Å in reedmergnerite (cf. Fig. 1 of Fleet, 1991a).

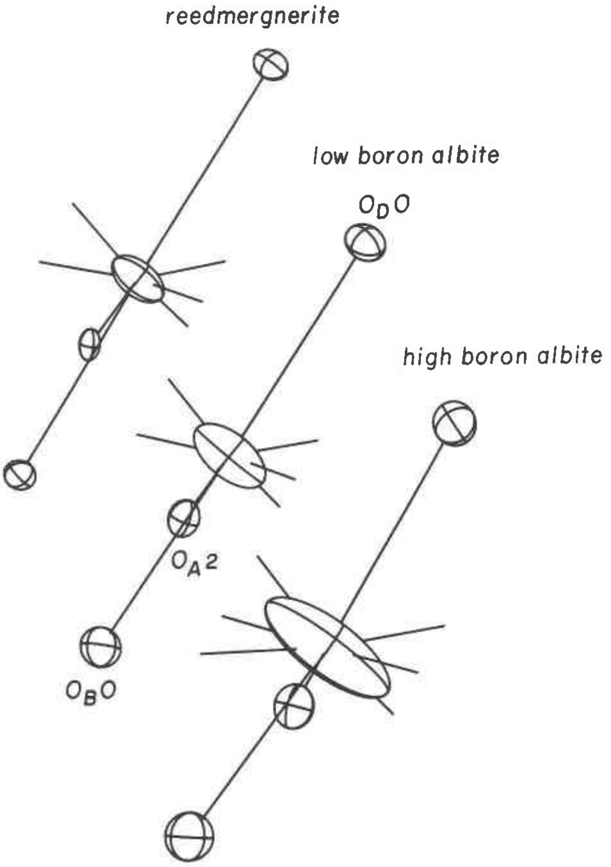

Fig. 2. Progressive increase in anisotropy of computed thermal ellipsoid of Na normal to plane of strongest Na-O bonds in reedmergnerite, low boron albite, and high boron albite (see Fig. 1 for complete stereochemical environment).

ally, with disorder of the tetrahedral-site atoms, the Na atom will experience static displacement along the major axis of the vibrational ellipsoid, stretching the strong bonds only marginally and forming shorter bonds with other proximal O atoms. The anisotropy of the "thermal" motion in albite structures should increase systematically with disorder (from ideally ordered to incipiently disordered to largely disordered). This prediction is illustrated in the present study, with the progression from reedmergnerite to low boron albite to high boron albite (Fig. 2).

The refined structure of low boron albite is comparable to that of reedmergnerite, with allowance for the small amount of tetrahedral-site disorder in the former (Table 7), which modifies T-O distances (Table 5) and increases all isotropic thermal parameters (Table 2). The refined structure of high boron albite (Tables 2 and 3) is comparable to that of high albite at room temperature (Prewitt et al., 1976) and that of disordered germanium albite (Fleet, 1991a), with allowance for the differences in ideal B-O, Al-O, Si-O, and Ge-O bond distances. O (T-O-T)

Table 7. Tetrahedral-site occupancies for reedmergnerite, boron albite, and other alkali feldspars

	Reference	T atom	$t_1$0	t_1m	$t_2$0	t_2m
Reedmergnerite	1	B	1.0	0.0	0.0	0.0
Low boron albite, Gb100	1	B	0.805(1)	0.014(1)	0.135(1)	0.046(1)
High boron albite, Gb87	1	B	0.289(3)	0.058(3)	0.384(3)	0.269(3)
Low albite	2	Al	0.97	0.04	0.0	0.0
Gallium albite	3	Ga	0.935	0.016	0.025	0.025
Gallium albite	4	Ga	0.887	0.031	0.044	0.038
$Al_{90}Ga_{10}$ albite	5	Ga	0.712	0.004	0.139	0.145*
$Al_{70}Ga_{30}$ albite	5	Ga	0.558	0.055	0.177	0.211*
Intermediate albite	6	Al	0.510	0.155	0.164	0.171
High albite	7	Al	0.28	0.25	0.22	0.25
Germanium albite	4	Al	0.274	0.375	0.185	0.166
Germanium albite	8	Al	0.212	0.436	0.150	0.202
Low sanidine	9	Al	0.345		0.125	

Note: References: 1 = present study; 2 = Harlow and Brown (1980); 3 = Fleet (1991a); 4 = Swanson (1986); 5 = Fleet (1991b); 6 = Phillips et al. (1989); 7 = Ribbe et al. (1969); 8 = Kroll et al. (1991); 9 = Colville and Ribbe (1968).

* Total Ga cations 0.1 and 0.3, respectively; occupancies normalized to $\Sigma t_i = 1.0$.

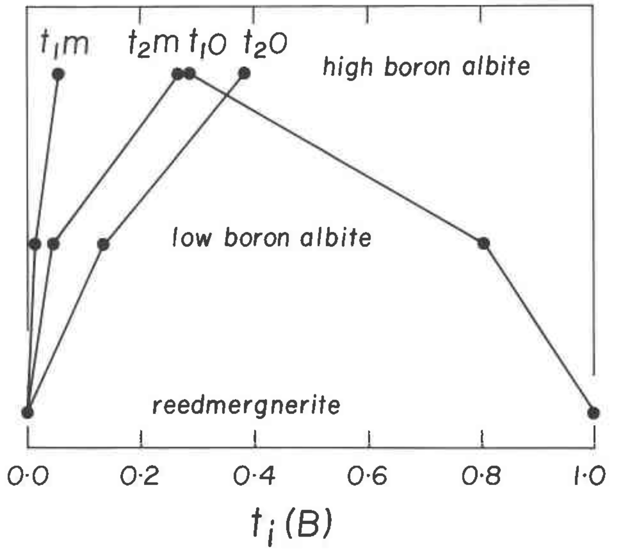

Fig. 3. Tetrahedral-site occupancies of B (t_iB) in reedmergnerite, low boron albite, and high boron albite. The lines connecting points in Figures 3 and 4 emphasize trends but do not imply that a continuous ordering path is necessarily present.

bond angles for these feldspar structures are compared in Table 6 (cf. Fleet, 1991a).

Tetrahedral-site occupancies

Tetrahedral-site occupancies for B (t_iB) in reedmergnerite and low and high boron albite are given in Table 7 and Figure 3. Whereas reedmergnerite is effectively ideally ordered, the low boron albite is incipiently disordered with a significant amount of B in T_20 and the site-preference sequence $t_10 \gg t_20 \gg t_2m > t_1m$. This site preference is maintained with increase in B-Si disorder (Fig. 3). In high boron albite, B is enriched in T_20 and depleted in T_1m. Thus, the tetrahedral-site ordering in boron albite is very unusual compared with albite ($NaAlSi_3O_8$). The site preference in high boron albite, with B favoring T_20 and Si strongly ordered in T_1m, is essentially opposite to that of germanium albite (Table 7), but depletion of the trivalent cation (and enrichment of Si) in T_1m is similar to the site ordering in Ga-substituted albite (Fleet, 1991b). The depletion of B in T_1m is so strong that high boron albite is antiordered in equivalent monoclinic symmetry [$t_1B = 0.17 < t_2B = 0.33$; Z negative (Thompson et al., 1974)].

The approximately linear correlations between average tetrahedral bond distance and Al-site occupancy in alkali feldspars are well established (e.g., Kroll and Ribbe, 1987). The present limited structural data for reedmergnerite and boron albite exhibit a good correlation between ⟨T-O⟩ and t_iB (Fig. 4). The values for T_10, T_20, and T_2m form a single curvilinear distribution, whereas the values for T_1m, which Fleet (1991a) noted has the smallest average T-O distance in low albite, low gallium albite, and reedmergnerite, appear to represent a separate distribution.

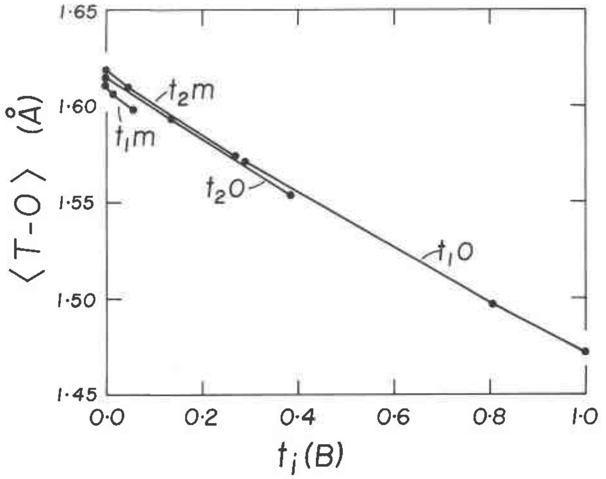

Fig. 4. Variation of average tetrahedral bond distance (⟨T-O⟩) with site occupancy of B (t_iB) in reedmergnerite and boron albite.

The excellent correlation between ⟨T-O⟩ and t_iB serves to confirm the present values for the refined tetrahedral-site occupancies.

The unit-cell parameters also correlate with change in site occupancies in boron albite. However, the shifts in parameters with order-disorder are each opposite to those in albite feldspars (see also Mason, 1980b). This is because Si is larger than B but smaller than Al. Thus, ⟨T_10-O⟩ is appreciably smaller than ⟨T(Si)-O⟩ in low boron albite but greater than ⟨T(Si)-O⟩ in low albite. Whereas the disordered structures of $NaBSi_3O_8$ and $NaAlSi_3O_8$ albites are dimensionally analogous, the dimensional distortions to transform to low boron albite and low albite, respectively, are of opposite sign. The angle γ of the present high boron albite is somewhat larger than that reported by Bruno and Pentinghaus (1974), 90.60 compared with 90.32°, indicating greater disorder in their material (see below).

Stability, synthesis, and order-disorder

Reedmergnerite and alkali feldspars from the Green River Formation are generally considered to be authigenic phases (Milton et al., 1954, 1960; Desborough, 1975). Whereas the present reedmergnerite is essentially ideally ordered, authigenic albite from the Green River Formation has only intermediate states of order (Desborough, 1975). In comparison, authigenic albite from marine limestones and dolostones is more ordered but seemingly not as ordered as low albite from low-grade (and very low grade) metamorphic rocks (Kastner, 1971). Although the controls on ordering in Na-Al albite remain controversial, the association of fully ordered reedmergnerite with intermediate ordered albite is qualitatively consistent with the preference sequence of trivalent substituents for the T_10 site of alkali feldspars ($Fe^{3+} > Ga > B > Al$; Fleet, 1991a). On the basis of the crystal-chemical behavior of $^{[4]}B$, $^{[4]}Al$, and $^{[4]}Si$ and the rate of ordering under laboratory conditions (e.g., ready synthesis of low boron albite at low P_{H_2O}), reedmergnerite would be expected to be more ordered than albite under authigenic conditions, where equilibrium may not be achieved. However, in view of the probable lower temperature for the order-disorder transformation in boron albite (see below), the relative state of ordering of reedmergnerite and albite in pegmatites is debatable.

The presence of quartz in the experimental products is consistent with disproportionation and the incongruent melting reported by Eugster and McIver (1959); the amount of quartz was proportional to the amount of H_2O added. The present experiments synthesized both low and high forms of boron albite and more closely defined the temperature of the order-disorder transformation. On the basis of the synthesis of low boron albite at 500 °C and 2.0 kbar by Eugster and McIver (1959), the synthesis of high boron albite at 700 °C, 4 bars by Bruno and Pentinghaus (1974), and his transformation of low to high boron albite at 830 °C, Kimata (1977) suggested that the transformation temperature is between 500 and 700 °C. In the present study, all single-crystal feldspar products grown on a cooling gradient from above 500 °C were high boron albite. Eugster and McIver (1959) reported incongruent melting to quartz + liquid (melt) at 567 °C, $P_{H_2O} = 1.0$ kbar and at 516 °C, $P_{H_2O} = 2.0$ kbar. In numerous experiments of the present study, glass was a common product for quench temperatures at or slightly above 500 °C. Thus, high boron albite may have nucleated at or below 550 °C in some of these experiments. Correspondingly, low boron albite was formed only in experiments maintained at or below 500 °C. Therefore, the order-disorder transformation in boron albite may be within the range 500–550 °C.

Further experimentation to bracket more closely the transformation temperature was beyond the scope of the present study. Although the high boron albite material presently studied was annealed at 478 °C, in retrospect it is considered unlikely that significant ordering was introduced after crystal growth. Under laboratory conditions, the rate of order-disorder of all feldspar materials in the solid state at low pressure is extremely low (cf. Martin, 1974; Goldsmith and Jenkins, 1985; Burns and Fleet, 1990). Solid-state diffusion is promoted by very fine grain size (Burns and Fleet, 1990), mineralizers (Martin, 1974), and high pressure in the presence of sodium carbonate (Goldsmith and Jenkins, 1985). This evidence suggests that under laboratory conditions even solid state processes in alkali feldspars are initiated at grain boundaries.

In this study the estimated temperature range for the order-disorder transformation in boron albite is lower than that for gallium albite (890–970 °C; Burns and Fleet, 1990) and albite (660–700 °C; Raase, 1971; Goldsmith and Jenkins, 1985). Interestingly, the sequence for T_10 site preference in these materials (Fe^{3+} > Ga > B > Al) does not correlate on a one-to-one basis with transformation temperature. The transformation in boron albite is rather abrupt and could be of first order under laboratory conditions; for example, Mason's (1980a, 1980b) observations point strongly to a recrystallization mechanism. However, because the order-disorder transformation is continuous in gallium albite (Burns and Fleet, 1990) and albite (at least at high pressure; Goldsmith and Jenkins, 1985), it may be continuous in reedmergnerite (natural $NaBSi_3O_8$) as well.

Crystal-chemical controls on ordering

The additional tetrahedral-site preferences revealed by study of analogue and substituted feldspars (Fleet, 1991a, 1991b; Kroll et al., 1991; present study) allow a more complete understanding of the crystal-chemical controls on ordering in alkali feldspars. The incompletely ordered and disordered materials are particularly important in this respect. Fleet (1991a) emphasized the role of spatial accommodation of the Na cation within the feldspar framework in defining the distinctive stereochemistries of the tetrahedral sites, particularly of T_10 and T_1m. It was tentatively concluded that the ordering scheme is determined by the favorable charge or valence-electron distribution resulting when the trivalent cation occupies T_10 and that this site preference is proportional to absolute difference in size with the quadrivalent cation.

As reviewed by Smith (1974), site ordering in monoclinic alkali feldspar is readily attributable to the favorable charge balancing of Al by Na when the former is ordered into the T_1 site. Fleet (1991a) noted that this favorable stereochemical relationship is maintained for T_10 in triclinic albite but not for T_1m. In fact, the distortion required to accommodate Na in low albite structures causes T_1m to be less favorable for the trivalent cation, in respect to proximity to Na, than T_20 and T_2m (e.g., Fig. 1). Crimping of the framework in the plane of strongest Na-O bonds (particularly at O atoms, O_B0 and O_D0) forces T_1m away from Na. This relative isolation of T_1m would explain the marked preference of Si for that site in Ga-substituted albite and boron albite. Fleet (1991b) concluded that the tetrahedral-site preference of Ga in sodium aluminum gallium feldspars is determined largely by the stereochemical association with nearest-neighbor (O) atoms. If next-nearest-neighbor tetrahedral atoms were a critical factor in determining site preference in alkali feldspars, in ordered albite structures the quadrivalent cation should exhibit a stronger preference for T_2m, which has two next-nearest-neighbor trivalent cations, than T_20. Nevertheless, favorable charge balancing through next-nearest-neighbors is a possible explanation for the preference of Si for T_2m and B for T_20 in boron albite (Table 7).

Several studies have suggested the importance of O bond angles (T-O-T) in controlling site preference in alkali feldspars (e.g., Brown and Gibbs, 1970; Smith, 1974; Geisinger et al., 1985; Kroll et al., 1991); these studies found Si favoring tetrahedra with wide O bond angles and B and Ge favoring tetrahedra with small angles. Kroll et al. (1991) pointed out that this correlation suggests an explanation for the antiordered site preference in germanium albite, Ge favoring T_10 (⟨T-O-T⟩ = 131.6°) and Al T_1m (⟨T-O-T⟩ = 144.0°). This suggests that in germanium albite the stabilization associated with optimization of O bond angles far outweighs that from favorable charge balancing. As noted above, the contribution of the latter when Al is in the T_1m site is minimal.

The correlation between site preference and average O bond angle may be extended to gallium albite and boron albite (Tables 6 and 7) because Ga and B both favor tetrahedra with small O bond angles (cf. Klaska, 1974; Fleet, 1987; Geisinger et al., 1985), and ⟨T-O-T⟩ = 132.5° and 136.0° for T_10 in low gallium albite and low boron albite, respectively. Also, Si shows the highest preference for T_1m, for which ⟨T-O-T⟩ = 148.2° and 145.7° in low gallium albite and low boron albite, respectively. However, the above explanations related to balancing valence requirements, proximity to Na, and spatial accommodation appear to be more appropriate for gallium albite and boron albite.

O bond angles in albite structures are largely defined by the accommodation of Na (e.g., Fleet, 1991a) and cation repulsion rather than the nature of the T-O bonding processes. The correlation between average bond angle and site preference can be rationalized on electrostatic grounds as well as from covalent bond theory, for example, strong repulsion of proximal Si cations, longer T-O bond distances for Ga and Ge, and screening of the residual charge on the small B cation by the surrounding O atoms. However, tetrahedral-site ordering patterns are strongly influenced by the stabilization afforded when the trivalent and quadrivalent cations are placed in the most appropriate stereochemical environments, and the O bond angle correlation, regardless of its physical basis, is certainly useful for qualitative understanding of site preference.

In germanium albite, the small difference in size between Ge and Al diminishes the tendency for ordering of the tetrahedral cations (Fleet, 1991a). Charge balancing through Na is apparently not a critical factor, and the stabilization related (directly or indirectly) to O bond angles determines the weak preference of Ge for T_10. In silicate albites, on the other hand, the competing effects of charge balancing requirements, atomic size difference, and T-Na and T-T repulsion appear to predominate.

ACKNOWLEDGMENTS

I thank G.E. Harlow and M.W. Phillips for constructive reviews of the manuscript, J.M. Hughes for editorial assistance, P.J. Dunn for provision of the specimen of reedmergnerite, F.J. Longstaffe for helpful discussion, and the Natural Sciences and Engineering Research Council of Canada for financial support.

REFERENCES CITED

Appleman, D.E., and Clark, J.R. (1965) Crystal structure of reedmergnerite, a boron albite, and its relation to feldspar crystal chemistry. American Mineralogist, 50, 1827–1850.

Brown, G.E., and Gibbs, G.V. (1970) Stereochemistry and ordering in the tetrahedral portion of silicates. American Mineralogist, 55, 1587–1607.

Bruno, E., and Pentinghaus, H. (1974) Substitution of cations in natural and synthetic feldspars. In W.S. MacKenzie and J. Zussman, Eds., The feldspars, p. 574–609. University Press, Manchester, England.

Burns, P.C., and Fleet, M.E. (1990) Unit-cell dimensions and tetrahedral-site ordering in synthetic gallium albite ($NaGaSi_3O_8$). Physics and Chemistry of Minerals, 17, 108–116.

Colville, A.A., and Ribbe, P.H. (1968) The crystal structure of an adularia and a refinement of the structure of orthoclase. American Mineralogist, 53, 25–37.

Desborough, G.A. (1975) Authigenic albite and potassium feldspar in the Green River Formation, Colorado and Wyoming. American Mineralogist, 60, 235–239.

Dusmatov, V.D., Popova, A.N., and Kabanova, L.K. (1967) The first occurrence of reedmergnerite in Russia. Doklady Akademie Nauk Tadzhikistan SSR, 10, 51–54.

Eugster, H.P., and McIver, N.L. (1959) Boron analogues of alkali feldspars and related silicates. Geological Society of America Bulletin, 70, 1598–1599.

Fleet, M.E. (1987) Crystal structures of α-$LiGaSiO_4$, α-$LiAlGeO_4$, and α-$LiGaGeO_4$. Zeitschrift für Kristallographie, 180, 63–75.

——— (1990) Gallium, aluminum-gallium, and germanium albite: Tetrahedral-site ordering in sodium feldspar. Geological Society of America Annual Meeting, Abstracts with Programs, A215.

——— (1991a) Structures of low gallium albite ($NaGaSi_3O_8$) and intermediate germanium albite ($NaAlGe_3O_8$): Tetrahedral-site ordering in sodium feldspar. American Mineralogist, 76, 92–99.

——— (1991b) Tetrahedral-site occupancies in sodium aluminum-gallium feldspar solid solutions [$Na(Al_{1-X}Ga_X)Si_3O_8$]. Journal of Solid State Chemistry, 92, 295–300.

Geisinger, K.L., Gibbs, G.V., and Navrotsky, A. (1985) A molecular orbital study of bond length and angle variations in framework structures. Physics and Chemistry of Minerals, 11, 266–283.

Ghose, S., and Wan, C. (1979) Hilgardite, $Ca_2[B_5O_9]Cl\cdot H_2O$: A piezoelectric zeolite-type pentaborate. American Mineralogist, 64, 187–195.

Goldsmith, J.R., and Jenkins, D.M. (1985) The high-low albite relations revealed by reversal of degree of order at high pressures. American Mineralogist, 70, 911–923.

Hamilton, W.C. (1965) Significance tests on the crystallographic *R* factor. Acta Crystallographica, 18, 502–510.

Harlow, G.E., and Brown, G.E., Jr. (1980) Low albite: An X-ray and neutron diffraction study. American Mineralogist, 65, 986–995.

Ibers, J.A., and Hamilton, W.C., Eds. (1974) International tables for X-ray crystallography, vol. 4. Kynoch Press, Birmingham, England.

Kastner, M. (1971) Authigenic feldspars in carbonate rocks. American Mineralogist, 56, 1403–1442.

Kimata, M. (1977) Synthesis and properties of reedmergnerite. Journal of Japanese Association of Mineralogy, Petrology and Economic Geology, 72, 162–172.

Klaska, K.-H. (1974) Strukturuntersuchungen an Tridymitabkommlingen (Beryllonitreihe, Trinephelin), 103 p. Ph.D. dissertation, University of Hamburg, Hamburg, Germany.

Kroll, H., and Ribbe, P.H. (1987) Determining (Al,Si) distribution and strain in alkali feldspars using lattice parameters and diffraction-peak positions: A review. American Mineralogist, 72, 491–506.

Kroll, H., Flogel, F., Breit, U., and Lons, J. (1991) Order and anti-order in Ge-substituted alkali feldspars. European Journal of Mineralogy, in press.

Martin, R.F. (1974) Controls of ordering and subsolidus phase relations in the alkali feldspars. In W.S. MacKenzie and J. Zussman, Eds., The feldspars, p. 313–336. University Press, Manchester, England.

Mason, R.A. (1980a) Changes in the crystal morphology of synthetic reedmergnerite ($NaBSi_3O_8$) during ordering experiments. Mineralogical Magazine, 43, 905–908.

——— (1980b) The ordering behaviour of reedmergnerite, $NaBSi_3O_8$. Contributions to Mineralogy and Petrology, 72, 329–333.

Milton, C., Axelrod, J.M., and Grimaldi, F.S. (1954) New minerals, reedmergnerite ($Na_2O\cdot B_2O_3\cdot 6SiO_2$) and eitelite ($Na_2O\cdot MgO\cdot 2CO_2$), associated with leucosphenite, shortite, searlesite, and crocidolite in the Green River formation, Utah. Geological Society of America Bulletin, 65, 1286–1287.

Milton, C., Chao, E.C.T., Axelrod, J.M., and Grimaldi, F.S. (1960) Reedmergnerite, $NaBSi_3O_8$, the boron analogue of albite, from the Green River Formation, Utah. American Mineralogist, 45, 188–199.

Ostertag, M. (1980) Synthese des Natrium-Bor-Feldspats $NaBSi_3O_8$ und Untersuchung des B,Si-Ordnungs-Unordnungsverhaltens in Abhangigkeit von Temperatur, Druck und Zeit. Diplomarbeit University of Munster, Munster, Germany.

Phillips, M.W., Ribbe, P.H., and Pinkerton, A.A. (1989) Structure of intermediate albite, $NaAlSi_3O_8$. Acta Crystallographica, C45, 542–545.

Prewitt, C.T., Sueno, S., and Papike, J.J. (1976) The crystal structures of high albite and monalbite at high temperatures. American Mineralogist, 61, 1213–1225.

Raase, P. (1971) Zur Synthese und Stabilitat der Albit-Modifikationen. Tschermaks Mineralogische und Petrographische Mitteilungen, 16, 136–155.

Ribbe, P.H., Megaw, H.D., Taylor, W.H., Ferguson, R.B., and Traill, R.J. (1969) The albite structures. Acta Crystallographica, B25, 1503–1518.

Sasaki, S., Fujino, K., Takéuchi, Y., and Sadanaga, R. (1980) On the estimation of atomic charges by the X-ray method for some oxides and silicates. Acta Crystallographica, A36, 904–915.

Smith, J.V. (1974) Feldspar minerals, vol. 1. Springer-Verlag, Berlin.

Swanson, D.K. (1986) High-temperature crystal chemical formalisms applied to $K_2Si^{VI}Si_3{}^{IV}O_9$ and $NaGaSi_3O_8$. Ph.D. thesis, State University of New York, Stony Brook, New York.

Thompson, J.B., Jr., Waldbaum, D.R., and Hovis, G.L. (1974) Thermodynamic properties related to ordering in end-member alkali feldspars. In W.S. MacKenzie and J. Zussman, Eds., The feldspars, p. 218–248. University Press, Manchester, England.

Manuscript received May 3, 1991
Manuscript accepted September 9, 1991